PCCP

Accepted Manuscript

www.rsc.org/pccp

Anion Exchange in Ionic Liquid Mixtures

Seoncheol Cha[1] and Doseok Kim[1]

[1]Department of Physics, Research Institute for Basic Science, Sogang University, 121-742, Republic of Korea

Abstract

Advantage of ionic liquids as designer solvents can be maximized by mixing different ionic liquids (ILs) for a possibility of continuous tunability of material properties. The property of these mixed ILs would be determined by their microscopic conformation between cations and anions. The mixtures of two ILs having 1-butyl-3-methylimidaolium cation and different anions were investigated by IR and NMR spectroscopy, utilizing that the vibrational frequencies of the C-H stretching and bending modes of the most acidic proton in the imidazolium ring of the cation and NMR chemical shift for the corresponding proton were clearly distinct between the ILs having different anions. The IR absorption spectra of the IL mixtures at different concentrations were well-matched to weighted sums of the two spectra of the pure ILs. In contrast, the two distinct peaks in the NMR spectra of the pure ILs coalesced into a single peak, which shifted continuously following the relative portion of two different ILs in the mixture. IR spectroscopy in the optical frequency range seems to take the instantaneous snapshot of the cation-anion interaction, while NMR spectroscopy in the radio-frequency (~ 500 MHz) range samples over much longer timescale, enough for the cation to interact with different anion species in the mixture.

1. Introduction

Ionic liquids are materials consisting only of cations and anions, and exist in liquid state at room temperature. Possessing unique material properties such as low very pressure and chemical stability, they are expected to replace conventional organic materials in many applications. Moreover, ionic liquids are called “designer solvents” as their physiochemical properties can be tuned by selecting proper cation and anion. Recently, mixing different ionic liquids has been proposed as a way of taking full advantage of ionic liquids with a hope of fine-tuning their physiochemical properties.[1,2] Furthermore, the ionic liquid mixtures consisting of well-known cations and anions can avoid the regulation and the approval involved with new chemicals[3]. Indeed the ionic liquid mixtures have recently found applications as solvents for dissolution of materials,[4] rechargeable batteries,[5] dye-sensitized solar cells,[6–8] and fuel cells.[9]

Thus many studies have been performed to examine the physiochemical properties of ionic liquid mixtures such as surface tension,[10] thermal and electrical conductivity,[11] viscosity,[11–13] density,[12–15] and other thermodynamic properties.[16,17] Recently, Clough et al. investigated systematically the physiochemical properties of several ionic liquid mixtures, and found out that the properties of the mixtures investigated were close to those expected from an ideal mixing, which is entropy-driven without the enthalpy change and yields simple mixtures.[3,14] By contrast, a mixture system can be a double salt showing non-ideal change of physiochemical properties from pure substances.[2,18] In the double salt, a cation or an anion in the mixture is considered to interact with the different counterion species simultaneously. Identifying whether a specific mixture is a simple mixture or a double salt would be important as the microscopic structure determines the physiochemical properties of the ionic liquid mixtures.[2]

Structural heterogeneity has been another important issue regarding the microstructure of ionic liquid mixtures. Quitevis and the coworkers studied the microstructure of binary ionic liquid mixtures by using optical Kerr effect (OKE), and suggested that each ionic liquid in the mixture is segregated in nanodomains when the size difference of the anions consisting the mixture is large.[19,20] On the other hand, Andanson et al. did not see any evidence of the nanostructural organization in the OH stretch bands from the trace amount of water put in as probe molecules in several binary mixtures of ionic liquids.[21] Payal and Balasubramanian performed molecular dynamics (MD) simulations for 1-butyl-3-methylimudaozolium ($[BMIM]^+$) cations having different anions (Cl^-, PF_6^-, and BF_4^-) and could not find the evidence of clustering of the same anions.[22] Shimizu et al. studied ionic liquids of imidazolium cations having different alkyl chain lengths (n = 2, 6) and bis(trifluoromethanesulfonyl)imide ($[TFSI]^-$) anion by using MD simulations and observed the existence of polar and non-polar domains, similar to the case of neat ionic liquids.[23]

Several researchers have studied the relation between the physiochemical properties and the structures of the ionic liquid mixtures. Aparicio and Atilhan performed IR absorption experiments and MD simulations of several ionic liquid mixtures and suggested the ideal change of thermodynamic properties.[24] Kirchner and co-workers performed *ab initio* MD simulations for mixtures of 1-ethyl-3-methylimidazolium ($[EMIM]^+$) based ionic liquids to investigate the competition between Cl^- and SCN^- on the hydrogen bonding site in the cation.[25,26] Villar-Garcia et al. suggested the emergence of new electronic environment from binary mixtures of ionic liquids from their X-ray photoelectron spectroscopy (XPS) result.[27] Rudwig and the coworkers studied the binary mixtures of triethylammonium-based ionic liquids having methylsulfonate and triflate anions by using far-IR spectroscopy and MD simulations to propose non-ideal mixing behavior of the ionic liquid mixtures.[28,29]

In many ionic liquids such as imidazolium-based ionic liquids, the interaction between the cation and the anion can be quite specific, like hydrogen bonding between the most acidic proton in the cation and the anion. When a mixture is made from different anions but sharing the same cation, the nature of hydrogen bonding is crucial in determining the microscopic structure and the physiochemical properties of the mixture. The change in the microscopic conformation between the cation and the anion in bulk ionic liquid as dictated by the hydrogen bonding strength was studied by *ab initio* calculations,[30] far-IR spectroscopy,[31,32] and IR/NMR spectroscopy.[33,34] The effect of hydrogen bonding on the physiochemical properties, such as melting points and viscosity, was also investigated.[35,36] In spite of its importance in the role played in bulk ionic liquids, the hydrogen bonding in ionic liquid mixture systems has not been investigated carefully as yet.

IR and NMR spectroscopy were chosen here for probing the hydrogen bonding of ionic liquids as the proton attached to C(2) in the imidazolium cation is the most acidic (chemical structure in Fig. 1), C(2)-H stretch vibrational mode in the IR spectrum and chemical shift for that H(C2) proton in the NMR spectroscopy was found to change sensitively for different anions, thus worked as good indicators of the hydrogen bonding between the cation and the anion.[34] Watanabe and the coworkers found distinct N-H···anion hydrogen-bond features from diethylmethylammnium-based ionic liquids having different anions and utilized them to investigate the binary mixtures of ammonium-based ionic liquid by using IR and NMR spectroscopy.[9]

In this report we investigated the hydrogen-bonding structures in several ionic liquid mixtures by using IR and NMR spectroscopy. [BMIM]BF_4 and [BMIM][TFSI] were selected as weakly-interacting ionic liquids, and [BMIM]Cl and [BMIM]I were selected as strongly-interacting ionic liquids. The ionic liquid mixtures of weakly- and strongly-interacting ionic liquids, and a mixture of two strongly interacting ionic liquids were investigated. The characteristic peaks of the hydrogen bonding in the IR spectroscopy for pure ionic liquids seemed to be maintained with reduced intensity without frequency shift in the mixture. However, the NMR chemical shift of H(C2) was seen as a single peak that shifted continuously for ionic liquid mixtures following the fraction change in the mixture. Combination of these results suggested the upper and lower bounds of the interaction timescale between the cation and the anion before switching to different anion in the mixtures.

2. Results & Discussion

2.1. IR Spectra

IR spectra of the imidazolium-based ionic liquids from 725 to 925 cm^{-1} and 2800 to 3200 cm^{-1} were shown in Fig. 2 as these regions contain characteristic features for the imidazolium ionic liquids having different anions. For neat ionic liquids the peaks at ~ 750 cm^{-1} were assigned to in-plane bending vibrational modes of C(4,5)-H (γ_{ip}C(4,5)-H). The C(2)-H out-of-plane bending vibrational mode (γC(2)-H) of [BMIM]Cl is very broad (extending from 800 to ~ 925 cm^{-1}) while that for [BMIM]I and [BMIM]BF$_4$ is narrower (peak positions at 810 cm^{-1} and 850 cm^{-1}, respectively), all in agreement with the previous reports.[37,38] As the peak position changes of γ_{ip}C(4,5)-H for different anions were less than 4 cm^{-1}, we chose to monitor γC(2)-H that showed more distinct changes for different anions. The isosbestic points were clearly observed at 850 cm^{-1} for [BMIM]Cl/[BMIM]I mixtures, 830 cm^{-1} for [BMIM]I/[BMIM]BF$_4$, and 825 and 875 cm^{-1} for [BMIM]Cl/[BMIM]BF$_4$ mixtures for γC(2)-H. This result indicates that the γC(2)-H mode of these ionic liquid mixtures are the weighted sums of the neat IR spectra, and strongly suggests that the hydrogen bonding between the C(2)-H and the anion of the neat ionic liquids remains intact in the mixtures of these ionic liquids.

The methylene and methyl stretch vibration modes of the imidazolium cation from 2800 cm^{-1} to 3000 cm^{-1} were similar for all neat and binary mixtures of ionic liquids. Although the absorption strengths were different, the change in the peak positions were all very small. On the other hand, the bands above 3000 cm^{-1} are very different for different anions. They are C(2)-H and C(4,5)-H stretch vibration modes (νC(2)-H and νC(4,5)-H) of neat ionic liquids, and have been known as good indicators of hydrogen bonding strength between the cation and the anion, to allow the distinction between different anion species[34,38–40]. For example, the strong absorption bands around ~ 3040 cm^{-1} of [BMIM]Cl and ~ 3070 cm^{-1} for [BMIM]I are contributions from νC(2)-H (3018 cm^{-1} for [BMIM]Cl and 3032 cm^{-1} for [BMIM]I) and ν_{as}C(4,5)-H (3057 cm^{-1} for [BMIM]Cl and 3078 cm^{-1} for [BMIM]I). By contrast the absorption of νC(2)-H for 3114 cm^{-1} for [BMIM]BF$_4$ was very weak, while ν_{as}C(4,5)-H for 3122 cm^{-1} was clearly blueshifted as compared to those for [BMIM]Cl or [BMIM]I due to much weaker cation-anion interaction.[34] From Figs. 2(e) and (f), these characteristic peaks at ~ 3040 cm^{-1} of [BMIM]Cl and ~ 3070 cm^{-1} for [BMIM]I did not change in position for mixtures with [BMIM]BF$_4$ but decrease with the increase of [BMIM]BF$_4$ in the mixture, as the

[BMIM]BF_4 has negligible absorption from 3000 cm^{-1} to 3100 cm^{-1}.[34] It should be noted that this absorption decrease without the peak position change is clearly distinct from that observed from the same ionic liquids [BMIM]Cl and [BMIM]I upon dilution with water.[34], in which these peaks continuously blueshifted upon dilution indicating the gradual weakening of hydrogen bond strength by dilution with water. By contrast, the invariant peak position in Fig. 2 was explained with the model that the [BMIM] cation interacted exclusively with either I^-/Cl^- or BF_4^- but not with both anions simultaneously.

As shown in Fig. 2(d), the C(2)-H stretch band of pure [BMIM]Cl (blue line) was relatively redshifted as compared to that of [BMIM]I (red line) due to the stronger hydrogen bonding between the cation and the Cl^-. Upon close examination, this peak (C(2)-H of pure [BMIM]Cl) seemed to shift slightly with the increase in the fraction of [BMIM]I in the mixture. To check for this possibility quantitatively for the spectra of [BMIM]Cl/[BMIM]I mixtures was quite difficult and ambiguous as their peaks overlapped significantly. The proximity of the other CH_x peaks as well as the existence of the Fermi resonance mode (with the overtone of in-plane imidazolium ring mode) complicates the problem further.[37,41–43] Thus, the additivity parameter (AP) which is the difference between the simulated and the experimental results, introduced by Quitevis group[19,20], was chosen for analyzing these binary ionic liquid mixtures. The simulated spectra were the weighted-sums of the neat spectra as follows

$$S^{\mathrm{calc}}(\omega) = A_a S_a(\omega) + A_b S_b(\omega) \quad (1)$$

where A_x is the molar concentration of species x and S_x is the spectrum of the neat ionic liquid x. Dashed lines in Fig. 3(a) were drawn as the weighted-sums of pure [BMIM]Cl and [BMIM]I spectra ($S^{\mathrm{calc}}(\omega)$), and nicely matched the experimental spectra ($S^{\mathrm{exp}}(\omega)$). The additivity parameter was defined as

$$AP = \sqrt{}\left(\sum_{\omega}[S^{\mathrm{exp}}(\omega) - S^{\mathrm{calc}}(\omega)]^2\right), \qquad (2)$$

and plotted for different concentrations in Fig. 3(c). The x-axis was changed to M% defined as the molar concentration of mixture divided by the molar concentration of neat ionic liquids. The mixture of [BMIM]BF_4 and 1-octyl-3-methylimidazolium tetrafluoroborate ([OMIM]BF_4) was chosen as a reference sample to check for any deviations from experimental artifacts, such as the change of refractive indices of the samples, as the spectra for this mixture system (sharing the same anion but differed only in the alkyl chain length in the cation) changed linearly as reported previously for the pyridinum-based ionic liquids[24]. The additivity parameters changed similarly between 0.02 and 0.05 for the binary mixtures of [OMIM]BF_4/[BMIM]BF_4, [BMIM]Cl/[BMIM]BF_4, and [BMIM]Cl/[BMIM]I. This result suggests that the hydrogen-bonding between each cation-anion pair is intact for these binary mixtures of ionic liquids regardless of concentrations or anion type.

As the busy spectra in the CH_x range made the quantitative analyses of the νC(2)-H challenging, the isotope-substituted imidazolium cation at C(2)-H position ([d-BMIM]) was made to isolate the C(2)-H peak from the vibrational spectra in the CH_x region. As shown in Fig. 4, C(2)-D stretch vibration modes (νC(2)-D) in 2150 – 2400 cm^{-1} are clearly separated in [d-BMIM]-ionic liquids from the rest of the C-H modes existing in 2800 cm^{-1} – 3200 cm^{-1}. The peak positions of νC(2)-D were 2244 cm^{-1} for [d-BMIM]Cl, 2290 cm^{-1} for [d-BMIM]I, and 2348 cm^{-1} for [d-BMIM][TFSI], clearly distinct from each other[34,37]. The broad band between 3050 cm^{-1} and 3100 cm^{-1} in Fig. 2 for [BMIM] cation indeed consist not only of C(2)-H mode, but also of C(4,5)-H and presumably some Fermi resonance modes[37].

Both νC(2)-D of [d-BMIM]Cl/[d-BMIM][TFSI] mixtures (Fig. 4(a)) and [d-BMIM]I/[d-BMIM][TFSI] mixtures (Fig. 4(b)) were clearly seen as a combination of two bands, while it is less clear for [d-BMIM]Cl/[d-BMIM]I mixtures in Fig. 4(c). All the spectra in Fig. 5 were deconvolved by using two Voigt functions without changing the peak positions, except for a small peak shift of νC(2)-D of [d-BMIM]Cl peak in [d-BMIM]Cl/[d-BMIM][TFSI] mixtures. This distinguishability of νC(2)-D modes of the neat components indicates that each [BMIM] cation in the ionic liquid mixture is interacting exclusive with only one anion at a time, and even the distance between the H(C2) and the anion does not change with the concentration.[22,25] Figure 6 shows the area change of the νC(2)-D modes from the fitting. The peak area for [BMIM]Cl was almost 6 times larger than that for [d-BMIM][TFSI]. This demonstrates that the stronger hydrogen bonding not only redshifts the stretch vibration mode but also increases the dipole absorption of the mode.[34] All the areas of νC(2)-D modes change proportional to the molar concentration without showing any preference for specific anion species.

In triethylamonium-based ionic liquid mixtures having methylsulfonate and triflate anions, nonlinear change in the area ratio between the peaks characteristic of the hydrogen bonding was reported, which contrasts to our data in Fig. 6.[28] There are three hydrogen bonding sites in the SO_3 moiety of the methylsulfonate and the triflate anions. Thus the number of cations is smaller than the number of hydrogen bonding sites, and the strongly interacting methylsulfonate anion has more chance to make hydrogen bonding with the cation than the triflate anion.[29] By contrast, with our anions investigated the imidazolium cation interacts mainly with single anion, thus less preferred anion also has ample chance to make an ion-pair with the nearby cation.

From the previous XPS experiment, (anion-sensitive) N 1s peak of the imidazolium cation, and the chloride peak of the mixture of [OMIM] (1-octyl-3-methylimidazolium) with Cl/[TFSI] and Cl/[TfO] (trifluoromethanesulfonate) anions were shown to shift continuously with the change in the anion fraction[27]. This contrasts with our IR spectroscopic result in the νC(2)-D region which strongly suggests the specific hydrogen bonding in the mixture system. A couple of explanations are suggested below to account for the observation and the apparent disparity between the XPS and the IR experiments. First, the electronic structures measured by XPS is mainly influenced by Columbic interaction between molecules while less sensitive to hydrogen bonding as already reported from the invariance of the characteristic peak after the methylation of C(2)-H in the imidazolium ring[44]. Thus, rather than observing the specific interaction between and the cation and the anion, the peak shift of the XPS spectra would be a consequence of the average electronic property (e.g. polarizability) change due to the different anion fraction. Thus these two techniques might probe different aspects of the intermolecular interactions. Second, the resolution of their high-resolution XPS instrument was around 0.5 eV, while the difference of N(1) peak position between [OMIM][TFSI], [OMIM]Cl, and 1-octyl-3-methylimidaozlium [OMIM][TfO] was less than 1 eV. Thus it would be challenging to decide whether an observed XPS peak is a single-peak which shifts following the new electronic state reflecting the environment of the mixture, or a combination of two peaks as an ensemble average of the two different electronic states.

2.2. NMR spectra

The of H(C2) proton chemical shift (δH(C2)) also changes sensitively for different anions as shown in Fig. 7.[34,45] The δH(C2) of [BMIM]I was 9.3 ppm, and had shift downfield with increasing fraction of [BMIM]Cl up to10.3 ppm. The chemical shift for [BMIM]BF_4 was 8.5 ppm.[34] This behavior of single peak shifting continuously is clearly distinct from that shown in the IR spectra of νC(2)-H and γC(2)-H bands of the mixtures.

These contradictory results from IR and NMR experiments from the ionic liquid mixtures were explained in terms of very different time scales (inversely proportional to the optical- and the radio frequency (RF) for IR and NMR, respectively) as compared to the timescale of the exchange between two different chemical states. This has been well-established for the NMR spectroscopy,[46,47] and extended to the vibrational spectroscopy.[48,49] The dynamics of the association and the dissociation dynamics in inorganic salts and protonation of organic molecule were studied by Raman and nonlinear Raman spectroscopy.[50] The two NMR peaks for the pure samples separated by Δν will coalesce into a single peak for the dynamics of the system faster than the coalescence time ($(2^{1/2}\pi\Delta\nu)^{-1}$),[46,47] for which the time is around 0.6 ms for δH(C2) under the 500 MHz NMR for [BMIM]Cl/[BMIM]BF_4 mixtures. As this time is definitely longer than the expected ion-pair exchange time, it is natural that we observe a single peak in the NMR spectra from the ionic liquid mixtures.[46,47] Similarly, the two νC(2)-D peaks in the mixtures spectra indicate that the dynamics of the system is slower than 0.1 ps for [d-BMIM]Cl/[dBMIM][TFSI] mixtures (ΔνC(2)-D ~ 100 cm^{-1}).[48] Thus the NMR and IR experiments suggest upper- and lower bounds for the anion exchange timescale.

The capability of the traditional NMR technique for measuring the chemical exchange time is limited to sub-microseconds, and is not enough to measure the exact chemical exchange time of the ionic liquid mixtures[51]. 2-dimensional IR spectroscopy have been utilized to measure the ultrafast dynamics such as spectral diffusion and vibrational mode coupling from picoseconds to nanoseconds.[52–54], and applied to ionic liquids to see the structural reorganization[55]. This technique has also been used to probe the chemical exchange for solute-solvent association and the hydrogen-bond making and breaking in water,[52,54] and can be applied in the future to investigate the ionic liquid mixtures to find out the anion exchange time.

The δH(C2) of the mixtures of [BMIM]Cl with several different anions were plotted in Fig. 8(a). The chemical shift for [BMIM]Cl/[BMIM]I mixtures changes linearly, while the graphs for the other mixtures are convex downward (shown more clearly in the normalized graphs in Fig. 8(b)). The amount of nonlinearity (the curvature in Fig. 8) follows the same order as the difference of the hydrogen-bonding strength between the two anions, showing the most curvature for [BMIM]Cl/[BMIM]PF_6. In view of the report that related small non-ideality in several ionic liquid mixtures with the difference of hydrogen bonding basicity (Δβ) between the ions,[3] our NMR data can be considered in terms of Δβ between two anions as well. However, the challenge remains to explain this nonlinear chemical shift together with the linear change of the peak areas in the IR spectra in Fig. 6.

3. Summary

The binary mixtures of imidazolium-based ionic liquids were studied by using IR and NMR spectroscopy. The hydrogen bonds between the cation and the anion were identified by using the hydrogen-bond sensitive γC(2)-H, νC(2)-H, and νC(2)-D modes of the IR spectra and the δH(C2) of the NMR spectra. The result from the IR spectra of the mixtures demonstrated that the hydrogen bonding between the C(2)-H and the anion of the neat ionic liquids remains intact in the mixtures while the number of hydrogen bonds between the cation and different anions was proportional to the anion concentrations in the mixture during the IR timescale. As the exchange of the hydrogen bonding between the cation and the different anions is much faster than the detection timescale of NMR, only the single peak is seen in the NMR spectra to reflect the fast chemical exchange as compared to the NMR timescale. The NMR chemical shift with the concentration change deviated from the linear line when the two ionic liquids had bigger difference in the interaction strength.

Acknowledgement

This research is supported by the National Research Foundation Grant No. 2011-0017435, and by the Sogang University Research Grant of 2014 (201410043.01). We thank Masahito Oh-e at Sharp for his careful reading and comments on our manuscript.

Methods

Ionic liquids (ultrahigh grade) were purchased from C-TRI (Korea) and IOLITEC (Germany), and dried under vacuum oven at ~ 80˚C. [BMIM]Cl was used at supercooled state after heating on hot plate less than 100 ˚C. In the measurements of C-D stretching modes, [BMIM][TFSI] was used instead of [BMIM]BF_4 because H(C2) of [BMIM]BF_4 cannot be deuterated even after exposer to D_2O for several days.[34] [BMIM]Cl/[BMIM]I mixtures were isotopically substituted by D_2O (Sigma Aldrich, 99.9 atom %D) and [BMIM]Cl/[BMIM][TFSI] and [BMIM]I /[BMIM][TFSI] mixtures were isotopically substituted by CH_3OD (Sigma Aldrich, 99.5 atom % D) in 0.95 mf of solvents as previously reported.[34,37] Cary 660(Aglient) FT-IR with HATR (Pike, 10 reflection ZnSe) was used to measure C(2)-D vibrational modes and GladiATR (Pike, single reflection diamond) was used to measure the rest of the IR spectra. Water circulator was used to measure the IR spectra at 60 ˚C. NMR is measured by UNITY-INOVA 500(Varian) 500MHz spectrometer with a co-axial external reference tube.

Reference

1 H. Niedermeyer, J. P. Hallett, I. J. Villar-Garcia, P. A. Hunt and T. Welton, *Chem. Soc. Rev.*, 2012, **41**, 7780–7802.

2 G. Chatel, J. F. B. Pereira, V. Debbeti, H. Wanga and R. D. Rogers, *Green Chem.*, 2014, **16**, 2051–2083.

3 M. T. Clough, C. R. Crick, J. Gräsvik, P. A. Hunt, H. Niedermeyer, T. Welton and O. P. Whitaker, *Chem. Sci.*, 2015, **6**, 1101–1114.

4 W. Xiao, Q. Chen, Y. Wu, T. Wu and L. Dai, *Carbohydr. Polym.*, 2011, **83**, 233–238.

5 T. Kakibe, J. Hishii, N. Yoshimoto, M. Egashira and M. Morita, *J. Power Sources*, 2012, **203**, 195–200.

6 F. Hao, H. Lin, Y. Liu and J. Li, *Phys. Chem. Chem. Phys.*, 2011, **13**, 6416–6422.

7 F. Hao, H. Lin, J. Zhang and J. Li, *J. Power Sources*, 2011, **196**, 1645–1650.

8 J. Chen, T. Peng, W. Shi, R. Li and J. Xia, *Electrochim. Acta*, 2013, **107**, 231–237.

9 M. S. Miran, T. Yasuda, M. A. B. H. Susan, K. Dokko and M. Watanabe, *J. Phys. Chem. C*, 2014, **118**, 27631–27639.

10 M. Geppert-Rybczyńska, J. K. Lehmann, J. Safarov and A. Heintz, *J. Chem. Thermodyn.*, 2013, **62**, 104–110.

11 M. Montanino, M. Moreno, F. Alessandrini, G. B. Appetecchi, S. Passerini, Q. Zhou and W. a. Henderson, *Electrochim. Acta*, 2012, **60**, 163–169.

12 P. Navia, J. Troncoso and L. Romaní, *J. Solution Chem.*, 2008, **37**, 677–688.

13 M. Larriba, S. Garc, P. Navarro and F. Rodr, *J. Chem. Eng. Data*, 2012, **57**, 1318.

14 P. Navia, J. Troncoso and L. Romaní, *J. Chem. Eng. Data*, 2007, **52**, 1369–1374.

15 J. N. Canongia Lopes, T. C. Cordeiro, J. M. S. S. Esperança, H. J. R. Guedes, S. Huq, L. P. N. Rebelo and K. R. Seddon, *J. Phys. Chem. B*, 2005, **109**, 3519–3525.

16 G. Annat, M. Forsyth and D. R. Macfarlane, *J. Phys. Chem. B*, 2012.

17 M. Kunze, S. Jeong, E. Paillard, M. Winter and S. Passerini, 2010, **14**, 12364–12369.

18 K. F. Robert L. Peck , Norman G. Brink , Frederick A. Kuehl Jr., Edwin H. Flynn , Alphonse Walti, *J. Am. Chem. Soc.*, 1945, **67**, 1866–1867.

19 D. Xiao, J. R. Rajian, S. Li, R. A. Bartsch and E. L. Quitevis, *J. Phys. Chem. B*, 2006, **110**, 16174–16178.

20 D. Xiao, J. R. Rajian, L. G. Hines, S. Li, R. a Bartsch and E. L. Quitevis, *J. Phys. Chem. B*, 2008, **112**, 13316–13325.

21 J.-M. Andanson, M. J. Beier and A. Baiker, *J. Phys. Chem. Lett.*, 2011, **2**, 2959–2964.

22 R. S. Payal and S. Balasubramanian, *Phys. Chem. Chem. Phys.*, 2013, **15**, 21077–21083.

23 K. Shimizu, M. Tariq, L. P. N. Rebelo and J. N. C. Lopes, *J. Mol. Liq.*, 2010, **153**, 52–56.

24 S. Aparicio and M. Atilhan, *J. Phys. Chem. B*, 2012, **116**, 2526–2537.

25 M. Brüssel, M. Brehm, A. S. Pensado, F. Malberg, M. Ramzan, A. Stark and B. Kirchner, *Phys. Chem. Chem. Phys.*, 2012, **14**, 13204–13215.

26 M. Brüssel, M. Brehm, T. Voigt and B. Kirchner, *Phys. Chem. Chem. Phys.*, 2011, **13**, 13617–13620.

27 I. J. Villar-Garcia, K. R. J. Lovelock, S. Men and P. Licence, *Chem. Sci.*, 2014, **5**, 2573–2579.

28 K. Fumino, A. Bonsa, B. Golub, D. Paschek and R. Ludwig, *Chemphyschem*, 2015, **16**, 299–304.

29 D. Paschek, B. Golub and R. Ludwig, *Phys. Chem. Chem. Phys.*, 2015, **17**, 8431–8440.

30 K. Dong, S. Zhang, D. Wang and X. Yao, *J. Phys. Chem. A*, 2006, **110**, 9775–9782.

31 K. Fumino, A. Wulf and R. Ludwig, *Phys. Chem. Chem. Phys.*, 2009, **11**, 8790–8794.

32 A. Wulf, K. Fumino and R. Ludwig, *Angew. Chem. Int. Ed. Engl.*, 2010, **49**, 449–453.

33 T. Takamuku, H. Hoke, A. Idrissi, B. a Marekha, M. Moreau, Y. Honda, T. Umecky and T. Shimomura, *Phys. Chem. Chem. Phys.*, 2014, **16**, 23627–23638.

34 S. Cha, M. Ao, W. Sung, B. Moon, B. Ahlström, P. Johansson, Y. Ouchi and D. Kim, *Phys. Chem. Chem. Phys.*, 2014, **16**, 9591–9601.

35 K. Fumino, T. Peppel, M. Geppert-Rybczyńska, D. H. Zaitsau, J. K. Lehmann, S. P. Verevkin, M. Köckerling and R. Ludwig, *Phys. Chem. Chem. Phys.*, 2011, **13**, 14064–14075.

36 P. A. Hunt, *J. Phys. Chem. B*, 2007, **111**, 4844–4853.

37 J. Grondin, J.-C. Lassègues, D. Cavagnat, T. Buffeteau, P. Johansson and R. Holomb, *J. Raman Spectrosc.*, 2011, **42**, 733–743.

38 T. Yamada, Y. Tominari, S. Tanaka, M. Mizuno and K. Fukunaga, *Materials (Basel).*, 2014, **7**, 7409–7422.

39 Y. Jeon, J. Sung, C. Seo, H. Lim, H. Cheong, M. Kang, B. Moon, Y. Ouchi and D. Kim, *J. Phys. Chem. B*, 2008, **112**, 4735–4740.

40 J.-C. Lassègues, J. Grondin, D. Cavagnat and P. Johansson, *J. Phys. Chem. A*, 2010, **114**, 687–688.

41 J.-C. Lassègues, J. Grondin, D. Cavagnat and P. Johansson, *J. Phys. Chem. A*, 2009, **113**, 6419–6421.

42 C. Roth, S. Chatzipapadopoulos, D. Kerlé, F. Friedriszik, M. Lütgens, S. Lochbrunner, O. Kühn and R. Ludwig, *New J. Phys.*, 2012, **14**, 105026.

43 S. Chatzipapadopoulos, T. Zentel, R. Ludwig, M. Lütgens, S. Lochbrunner and O. Kühn, *ChemPhysChem*, 2015, **16**, 2519–2523.

44 T. Cremer, C. Kolbeck, K. R. J. Lovelock, N. Paape, R. Wölfel, P. S. Schulz, P. Wasserscheid, H. Weber, J. Thar, B. Kirchner, F. Maier and H. P. Steinrück, *Chem. - A Eur. J.*, 2010, **16**, 9018–9033.

45 A. Wulf, K. Fumino, D. Michalik and R. Ludwig, *ChemPhysChem*, 2007, **8**, 2265–2269.

46 J. Kaplan, *J. Chem. Phys.*, 1958, **28**, 278–282.

47 A. Carrington and A. D. McLachlan, *Introduction to Magnetic Resonance:with Applications to Chemistry and Chemical Physics*, Harper&Row, 1967.

48 R. A. MacPhail and H. L. Strauss, *J. Chem. Phys.*, 1985, **82**, 1156–1166.

49 B. Cohen and S. Weiss, *J. Chem. Phys.*, 1980, **72**, 6804.

50 H. Hamaguchi, *Frontiers of Molecular Spectroscopy*, Elsevier, 2009.

51 A. D. Bain, 2003, **43**, 63–103.

52 J. Zheng, K. Kwak, J. Asbury, X. Chen, I. R. Piletic and M. D. Fayer, *Science (80-.).*, 2005, **309**, 1338–1343.

53 M. R. Panman, C. N. van Dijk, H. Meuzelaar and S. Woutersen, *J. Chem. Phys.*, 2015, **142**, 041103.

54 Y. S. Kim and R. M. Hochstrasser, *Proc. Natl. Acad. Sci. U. S. A.*, 2005, **102**, 11185–11190.

55 Z. Ren, A. S. Ivanova, D. Couchot-Vore and S. Garrett-Roe, *J. Phys. Chem. Lett.*, 2014, **5**, 1541–1546.

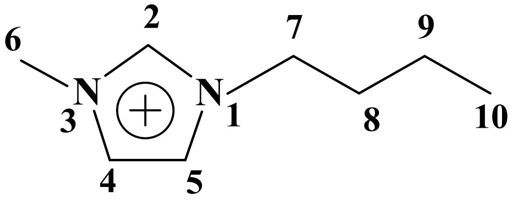

Figure 1. Chemical structure of the 1-butyl-3-methylimidazolium cation ($[BMIM]^+$)

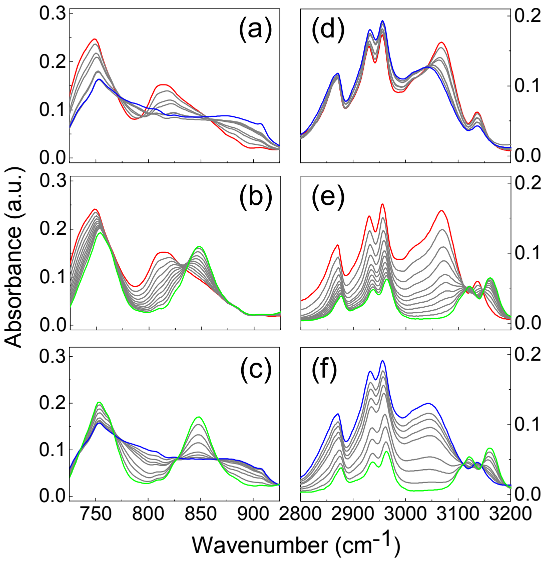

Figure 2. IR spectra of binary ionic liquids mixtures of [BMIM]X for (a)-(c) C(2)-H bending and (d)-(f) C(2)-H stretch vibrational modes. blue: [BMIM]Cl, red: [BMIM]I, green: [BMIM]BF_4. [BMIM]Cl/[BMIM]I mixture concentrations are 1, 0.90, 0.78, 0.63, 0.56, 0.34, 0.14, 0 mf (for [BMIM]Cl). [BMIM]I/[BMIM[BF_4 mixture concentrations are 1, 0.88, 0.77, 0.66, 0.56, 0.46, 0.36, 0.27, 0.18, 0.09, 0 mf (for [BMIM]I). [BMIM]Cl/[BMIM]BF_4 mixture concentrations are 1, 0.92, 0.88, 0.80, 0.75, 0.71, 0.61, 0.46, 0.30, 0.13, 0 mf (for [BMIM]Cl).

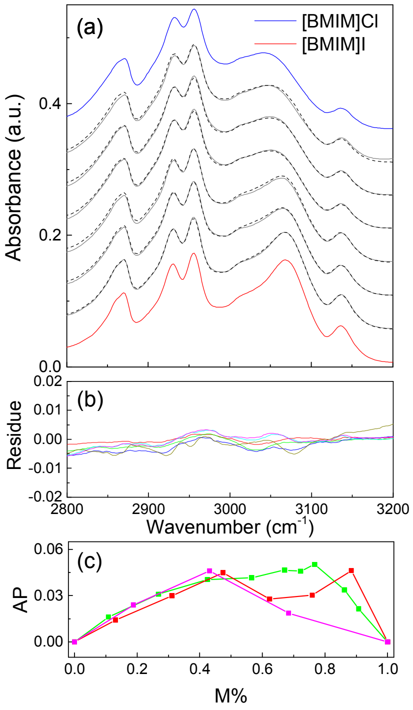

Figure 3. (a) Comparisons between the experimental (solid lines) and the simulated spectra (dotted lines, using eq. (1)) of [BMIM]Cl/[BMIM]I mixtures, and (b) their residuals. (c) AP (additivity parameter, using eq. (2)) of the several ionic liquid mixtures vs. the component fraction. [BMIM]Cl/[BMIM]BF_4 (green), [BMIM]Cl/[BMIM]I (red), and [BMIM]BF_4/[OMIM]BF_4 (magenta).

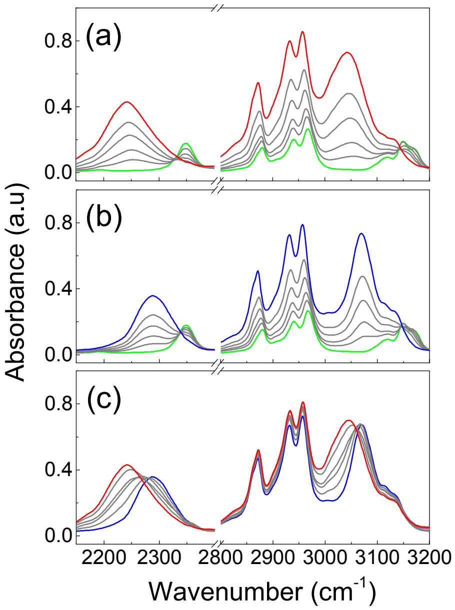

Figure 4. IR Spectra of C(2)-D and C-H vibration modes of (a) [BMIM]Cl/[BMIM][TFSI] and (b) [BMIM]I/[BMIM][TFSI], and (c) [BMIM]I/[BMIM]Cl mixtures, all for 0, 0.2, 0.4, 0,6, 0.8, 1.0 mf.

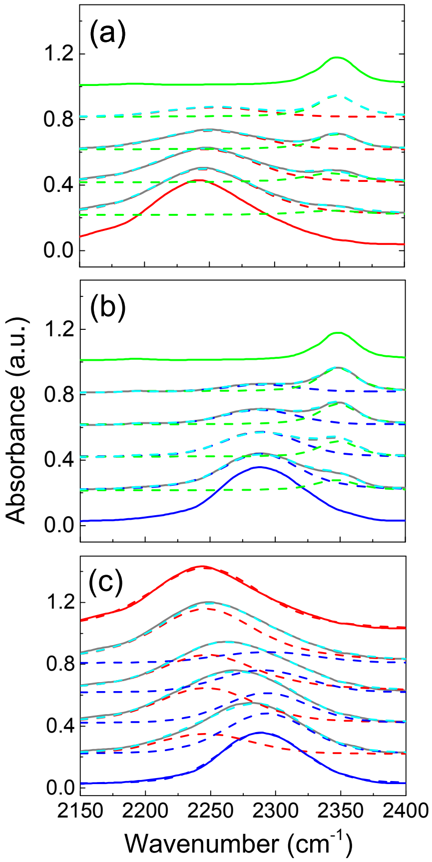

Figure 5. Comparisons between the experimental spectra (solid lines) and the fittings by using double Voigt functions (cyan dashed lines) for (a) [d-BMIM]Cl/[d-BMIM][TFSI], (b) [d-BMIM]I/[d-BMIM][TFSI], and (c) [d-BMIM]Cl/[d-BMIM]I. The green, red, and blue dashed lines are deconvolved Voigt function components.

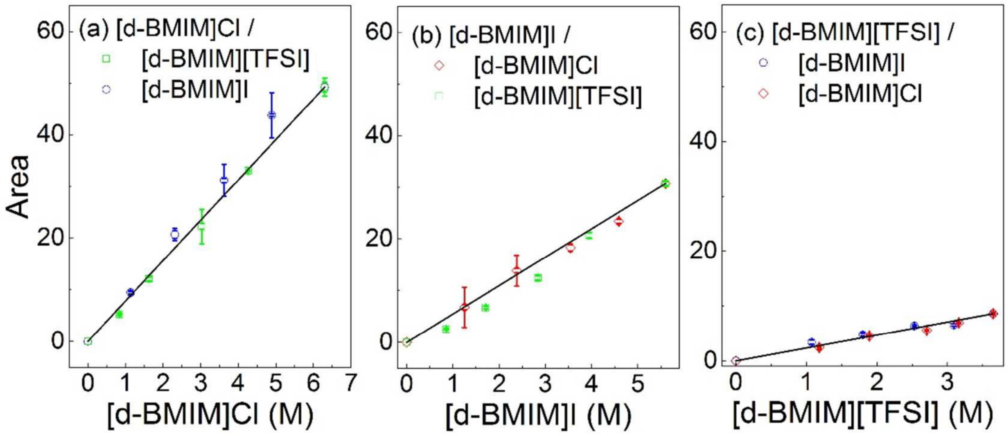

Figure 6. Peak area changes of νC(2)-D for (a) [BMIM]Cl, (b) [BMIM]I, and (c) [BMIM][TFSI] with the other ionic liquids.

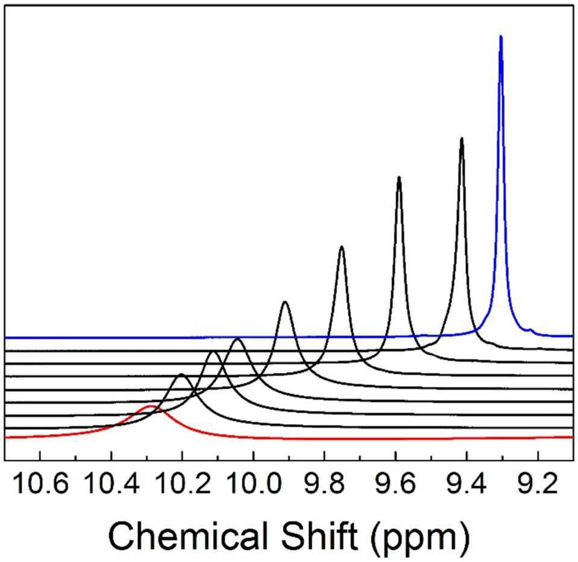

Figure 7. H(C2) proton chemical shift of [BMIM]Cl/[BMIM]I mixtures. (red: pure [BMIM]Cl, blue: pure [BMIM]I)

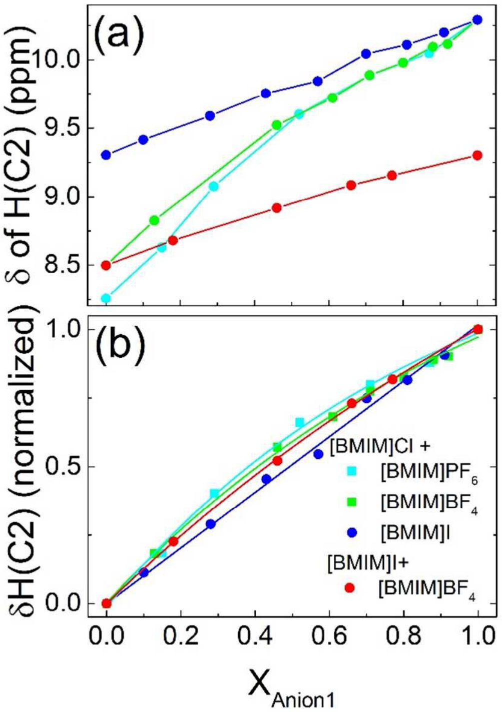

Figure 8. (a) Concentration dependent δ of ionic liquids mixtures and (b) the normalized chemical shifts. X_{Anion1} denotes the mole fractions of [BMIM]Cl for mixtures containing [BMIM]Cl, while it denotes the mole fraction of [BMIM]I only for [BMIM]I/[BMIM]BF_4 mixtures.